In vitro controlled release of extracellular vesicles for cardiac repair from poly(glycerol sebacate) acrylate-based polymers

Thomas Hamada, Julie L.N. Dubois, Valérie Bellamy, Laetitia Pidial, Albert Hagège, Maria N. Pereira, Philippe Menasché

In vitro controlled release of extracellular vesicles for cardiac repair from poly(glycerol sebacate) acrylate-based polymers

Thomas Hamada,[1,2] Julie L.N. Dubois,[1] Valérie Bellamy,[2] Laetitia Pidial,[2] Albert Hagège,[2,3] Maria N. Pereira,[1*] Philippe Menasché,[2,4*].

Affiliations

[1] TISSIUM SA, 74 rue du Faubourg Saint-Antoine, 75012 Paris, France.
[2] INSERM UMRS 970, Paris Centre de Recherche Cardiovasculaire (PARCC), Université de Paris, Paris, France.
[3] Department of Cardiology, Assistance Publique-Hôpitaux de Paris, Hôpital Européen Georges Pompidou, 20, rue Leblanc, 75015 Paris, France.
[4] Department of Cardiovascular Surgery, Assistance Publique-Hôpitaux de Paris, Hôpital Européen Georges Pompidou, 20, rue Leblanc, 75015 Paris, France.

*co-corresponding authors

Maria N. Pereira: TISSIUM SA, 74 rue du Faubourg Saint-Antoine, 75012 Paris, France;
Phone: +33 6 69 15 59 45; mail: mpereira@tissium.com

Philippe Menasché: Department of Cardiovascular Surgery, Hôpital Européen Georges Pompidou, 20, rue Leblanc, 75015 Paris, France.
Phone: +33156093622; mail: philippe.menasche@aphp.fr

Abstract

Cell therapy to restore cardiac function in chronic heart failure has been extensively studied. However, its therapeutic value is limited due to poor cell engraftment and survival and the therapeutic outcomes have been attributed to paracrine secretions such as extracellular vesicles (EV). The direct use of EV is an attractive therapeutic strategy and it has been shown that the kinetics of delivery of the EV to the targeted tissue may impact the outcomes. However, there are currently no technologies to deliver EV to the heart in a controlled and tunable manner. The objective of this study was to design a controlled release system, based on a photocurable adhesive polymer, to locally deliver EV to the cardiac tissue. We have first demonstrated that the adhesive polymer, PGSA-g-EG, did not impact the EV bioactivity *in vitro* and was biocompatible *in vivo* when tested in a rat model. Importantly, the polymer remained attached to the heart surface for at least 1 month. We have then evaluated and optimized the *in vitro* release kinetics of the EV from the PGSA-g-EG polymer. Freeze-dried EV formulations were developed to tune the release kinetics and maximize the loading in the polymeric material. Moreover, despite the instability of the EV in aqueous medium at 37°C, the PGSA-g-EG polymer was able to release bioactive EV for at least 14 days. Overall, these results suggest that the PGSA-g-EG is a suitable material to promote the controlled delivery of bioactive EV over an extended period of time.

Keywords

Extracellular Vesicles, Polymer formulation, Adhesive, Controlled Release, Chronic Heart Failure.

1. Introduction

Cardiovascular diseases are a leading cause of death worldwide [1]. Only in the United States, 1.5 million of cases of myocardial infarction (MI) occur every year [2]. During a MI, the sudden blockade and reduced blood flow in the coronary arteries [1] often lead to the irreversible necrosis of the heart muscle, which due to its poor regenerative capacity can result in chronic heart failure and patient's death [3,4]. The current standard of care aims to prevent/limit ischemic attacks, or to support function through mechanical assist devices [1]. However, these procedures are not consistently able to restore and repair the function of the cardiac tissue [5].

In recent years, stem or progenitor cells have gained considerable interest for the treatment of heart failure [6] because of their alleged potential to improve cardiac function through the regeneration of the cardiac tissue [7]. However, improvements, if any, reported by clinical trials have usually been modest [7–11]. Recent studies demonstrated that these cells tend to die quickly [12,13], suggesting that their benefits, if any, are more likely mediated by a paracrine activation of endogenous repair pathways by cell-released cytokines, growth factors and extracellular vesicles (EV) [14–16]. These EV are small bilipid membrane-bound particles with a heterogeneous and dynamic content [17–19] which can be isolated from all cells and biological fluids [20].

Several pre-clinical studies have been conducted to evaluate the therapeutic effect of EV derived from non-differentiated cells on heart function [21,22]. For example, recent studies showed, both *in vitro* and *in vivo* in different animal models, that human mesenchymal stem cells (hMSC)-derived EV are able to reduce myocardial ischemic injury through angiogenic and cardioprotective mechanisms [23–25]. Human induced pluripotent cardiac progenitors (iPSC-Pg) have also been shown to be effective [26–28]. The major mechanisms whereby EV are hypothesized to contribute to cardiac repair include mitigation of inflammation, apoptosis and fibrosis as well as stimulation of angiogenesis whereas induction of

proliferation of resident cardiomyocytes to increase the contractile pool remains more controversial [29].

Current EV delivery techniques are limited to systemic or local injections. However, even upon local injection, EV tend to diffuse quickly around the infarcted zone [30], thereby limiting the dose able to reach the diseased tissue. The need for regular injections to maximize treatment effects is a major challenge for the translation of these therapies [31]. For example, a recent investigation demonstrated the effect of weekly intra-articular injections of human MSC-derived EV to repair osteochondral defects in rat. After twelve weeks, new hyaline cartilage and subchondral bone, structurally similar to the original one, was observed [31]. Another study demonstrated the benefits of a hydrogel glue-based patch loaded with EV compared to short-term repeated injections in cartilage regeneration [32]. Thus, to improve the therapeutic potential of EV, local EV delivery devices may be required to maximize the EV concentration and long-term bioavailability in the targeted tissue [30,32,33]. Recently, a rat collagen patch within a GELFOAM^{TM} mesh loaded with EV derived from iPSC-derived cardiomyocytes was developed. This device was able to promote tissue regeneration and improve cardiac function [34]. Another study demonstrated that an injectable hyaluronic acid hydrogel loaded with EV derived from endothelial progenitor cells improved heart function recovery in a rat MI model [35]. No significant difference was reported compared to the same hydrogel loaded with endothelial progenitor cells.

In this study, we evaluated the potential of a new adhesive and photocurable polymeric material, based on poly(glycerol sebacate) acrylate polymer (PGSA) [36,37], to be used as a vehicle to deliver EV to the heart. Initially synthesized and characterized by Nijst *et al.* in 2007 [36], PGSA has been studied for multiple biomedical applications, including surgical glues [37,38] and scaffolding for tissue regeneration [39]. This polymer with tunable mechanical properties has been previously shown to be biocompatible and biodegradable. Furthermore, when delivered to tissue, it presents a minimum washout due to its hydrophobic and viscous nature and enables on-demand adhesion to biological tissues using light. We

hypothesize that these are core design criteria to maximize the delivery of EV to a dynamic tissue like the heart. In the present study, we selected a derivative of PGSA, Poly(glycerol-co-sebacate) acrylate ethylene glycol (PGSA-g-EG), which differs from previous hydrogels tested for the release of EV, and after having assessed *in vitro* its capacity to release bioactive EV in a controlled manner, we evaluated the biocompatibility and adhesion performance of the material in a rodent model.

2. Materials and Methods

2.1. Ethics section

All procedures were approved by our PARCC institutional ethics committee and complied with European legislation (European Commission Directive 86/609/ EEC) on animal care. All *in vitro* tests using human cells were carried out with the agreement of the donors who signed an informed consent.

2.2. Synthesis of PGSA-g-EG

Polyglycerol-*co*-sebacate (PGS) was synthesized through the polycondensation of glycerol and sebacic acid, as previously described [36]. Poly(glycerol-co-sebacate) acrylate ethylene glycol (PGSA-g-EG) was synthesized according to a protocol previously described with some modifications [40]. PGS (18.75 mmol) was solubilized in dichloromethane (300 mL) for 15 min under stirring and nitrogen atmosphere. Triethylamine (0.36 mmol), acetyl-chloride (0.15 mmol) and 2-methoxyethyl chloroformate (0.21 mmol) were added dropwise into the solution which was stirred overnight at room temperature in the dark. Ethanol (132 mL) was added into the flask and the mixture stirred for 24h at 40°C in the dark under nitrogen. The following day, the solvent was evaporated at 40°C using rotavapor (pressure 100 mbar, 25°C). The mixture was resuspended in ethyl acetate (300 mL) and washed three times with brine solution (3 x 100 mL). The organic phase was dried with magnesium sulfate and filtered. Ethyl acetate was evaporated using rotavapor (10 mbar, 40°C). The polymer was resuspended into dichloromethane to reach 50% (w/w) solution. The Irgacure TPO-loaded polymer was purified by supercritical carbon dioxide (by StaniNov® Technology) in aseptic

conditions. After purification, the polymer was characterized by ^{1}H-NMR, NMR DOSY (Diffusion Ordered Spectroscopy), gel permeation chromatography (GPC), Gas Chromatography - Flame Ionization Detector (GC-FID), and HPLC.

2.3. Production of EV from human iPS progenitor cells (iPSC-Pg)

The EV were produced as previously described [27].The cryo-conserved iPSC-Pg were thawed and seeded at a density of 78,000 cells/cm² on fibronectin-coated cell culture flasks according to the supplier information (Cellular Dynamics International, Madison, WI, USA). The cells were cultured for 4 days at 7% CO_2 and 37°C in William's E medium supplemented with B cocktail, gentamicin (25 µg/mL), human FGF-2 (1 µg/mL) and purified Bovine Serum Albumin (5% v/v). No Fetal Bovine Serum (FBS) was used in the cell culture medium. The major reason for discarding FBS and using BSA is that in contrast to the former (even if it is credited to be exosome-free), the latter does not yield particles which could be misinterpreted as extracellular vesicles by Nanoparticle Tracking Analysis (NTA).

The medium was removed after 2 days and replaced with fresh medium. The conditioned medium after 2 and 4 days of culture (loaded with the secreted EV) was collected. The medium was centrifuged for 10 min at room temperature (RT) at 300*g* to remove the cell debris and dead cells. The supernatant was collected and transferred in 50-mL centrifugal tubes and centrifuged again for 10 min at 400*g* at RT. The supernatant was collected, and a third step of centrifugation was performed for 30 min at 2,000*g* at RT. Collected media at day 2 and 4 were stored at -80°C until EV isolation by ultracentrifugation. The content of the iPSC-Pg-EV, as well as their biological mode of action, have previously been previously characterized and described by our group [27].

2.4. Isolation of EV

After thawing, the collected medium was transferred to ultracentrifugation tubes. For trehalose (TRE)-containing EV, filtered PBS supplemented with 80% (w/v) TRE was added to the collected medium. An ultracentrifugation at 100,000*g* for 16h at 4°C was carried out, after which the viscous pellet was collected. PBS or PBS supplemented with 2.5% or 10%

(w/v) TRE (100 µL) was used to rinse the ultracentrifugation tube. The solution was aliquoted and stored at -80°C until further use.

2.5. *In vitro* cytotoxicity of PGSA-g-EG

H9c2 rat cardiac myoblasts were seeded at 25,000 cells/cm² on 0.2% gelatin-coated plates. The medium used was DMEM + glutamax supplemented with 10% (v/v) FBS and 1% (v/v) PSA at 37°C and 5% CO_2. After 24h of cell culture (considered as T0), the cell culture medium was replaced by Fetal Bovine Serum-containing (DMEM 10%FBS, positive control), serum-free DMEM (negative control) or test items prepared as described in sections 2.5.1 and 2.5.2.

For the different conditions, after 27-h incubation, the number of cells was determined using cell counting Muse™ (0500-3115, Merck Millipore, Guyancourt, France) coupled with a viability kit (MCH100102, Merck Millipore). The number of cells was normalized against the cell number in serum-free DMEM. Each condition was evaluated in biological duplicates or triplicates and the experiments were performed at least 2 times.

2.5.1. *In vitro* cytotoxicity of PGSA-g-EG extracts.

Uncured PGSA-g-EG (15 mg) was incubated for two hours at RT in filtered PBS (80 µL). Polymer extracts were diluted at a concentration of 1% (v/v) in DMEM 10%FBS. After 24h of culture, H9c2 rat cardiac myoblasts were incubated with polymer extracts (considered as T0). After a 27-h incubation, the number of cells was determined using the protocol described above.

2.5.2. Impact of PGSA-g-EG on EV bioactivity

Uncured PGSA-g-EG (15 mg) was incubated for 2h at RT with EV solution (80 µL). After incubation, the solution of EV was diluted in serum free DMEM to reach $5x10^9$ EV/well. To determine the toxicity of PGSA-g-EG on EV, we evaluated their effect on H9c2 rat cardiac myoblast viability after serum deprivation. After 27h of incubation, the number of cells was counted using the protocol described above.

2.6. *In vivo* experiment to evaluate the PGSA-g-EG biocompatibility

Male Wistar rats (250 g) were anesthetized with 2%-3% isoflurane. Anesthesia level and temperature were monitored during the procedure. The rats were randomly assigned to implantation with *in situ* cured PGSA-g-EG while a second group served as sham-operated controls (no polymer implantation). After tracheal intubation, mechanical ventilation was set at a rate of 70 mL/min with a 2 mL average insufflation volume. The animals were kept on a heating pad and eye gel was added to prevent drying. The heart was exposed through a left thoracotomy. Warm (37°C) polymer was applied on the left ventricle using a 1mL syringe and 16 G catheter cut at 1cm-length, covering an area of 0.5cm x 1cm [27] and was cured using a LED 405 nm light source for 30 seconds at 130 mW/cm^2. The total surface area of the implant represented approximately 0.5 cm^2.

After the implantation and chest closure, the scar area was sprayed with a solution of xylocaine (10% v/v) in addition to buprenorphine injection (0.1 mg/kg). Following the surgery, animals were evaluated for weight loss, pain, prostration and wound healing.

Animals were sacrificed after 1 week and 1 month. Collected hearts were thoroughly cleaned with PBS to avoid blood clot formation. After removal of the atria, hearts were embedded in OCT medium and frozen in liquid nitrogen until histological analysis.

2.7. Histopathological analysis of the hearts

Histopathological analysis was performed by an independent blinded pathologist. Five-µm transverse sections were taken in the middle of the heart where the patch was applied. Sections were stained using Masson’s Trichrome (Weigert's hematoxylin, fuchsin acid, phosphomolybdic acid and Malachite green), and Hematoxylin Eosin Saffron (HES) staining. The analysis of the microscopic findings was divided in (1) chronic inflammation and (2) fibrosis and scored as following: Grade 1: Minimal /very few / very small; Grade 2: Slight / few/small ; Grade 3: Moderate/moderate number/moderate size ; Grade 4: Marked/many/ large ; Grade 5: Massive/extensive number/extensive size.

2.8. EV Formulations

2.8.1. Freeze-drying of EV

Equal volumes of EV were aliquoted and stored at −80°C for at least 24h. After flash freezing in liquid nitrogen for 5 min, frozen EV were freeze-dried using a CRIOS-85 (Cryotec, Montpellier, France) for 6 hours. Freeze-dried EV (FD EV) were stored at -80°C.

2.8.2. Stability of freeze-dried EV

To assess the stability of EV after release, we incubated the freeze-dried EV from 0 to 60 days at 37°C in aseptic conditions. The EV were resolubilized in the same volume of distilled water (100 µL) as prior to incubation. EV were then stored at -80°C until analysis.

Three different analyses were performed: bioactivity assays, structural observations (cryoTEM) and evaluation of the microRNA concentration.

2.8.3. Mixing of the PGSA-g-EG/EV formulations and EV release studies

An amount of 4.5 10^{10} EV was selected. To compensate for the weight differences between EV/2.5% TRE and EV alone, the loading percentage was adapted. With freeze-dried EV, 14% or 19% (w/w) loading were tested. The release of EV/2.5% TRE was also determined with two loading percentages: 19% and 28%. Warm PGSA-g-EG (42 to 100mg) was mixed with freeze-dried EV or EV 2.5% (w/w) TRE (6 to 20 mg). Six mm-diameter discs (thickness: 400 µm) were cured using a LED 405 nm light source at 130 mW/cm^2.

Three discs were incubated in 0.1 µm-filtrated PBS (200 µL) at 37°C and 100 rotations per minute. At defined time points, the PBS was collected and replaced by fresh PBS. The samples were kept at -80°C until their analysis.

2.8.4. EV release quantification

As previously described [27], the bioactivity of EV on H9c2 cells is concentration-dependent. This dose-bioactivity correlation was used as a calibration curve to determine the release kinetics from the different PGSA-g-EG formulations. The dose-effect can be mathematically represented by a second-degree polynomial like $y= a_2x^2 + a_1x + a_0$. A different calibration

equation was then performed for each replicate of the release experiments. For each number of cells (*y*) at the defined time point, the corresponding equation was solved using MATLAB® functions. Then an approximation of the released EV was determined.

2.9. Characterization of EV formulations

2.9.1. Quantification and size distribution of EV by NTA

After isolation, the EV were characterized by NTA using a Nanosight (NTA 3.2, LM-14; laser 488nm-Malvern Instruments Ltd., Malvern, United-Kingdom) to estimate the proportions of each EV sub-population (exosomes and microparticles) based on particle size. The analysis was carried out using a camera level setting to 15. During the image analysis, the detection threshold was set at 4. This threshold determined the minimal light quantity to consider a light dot as a positive signal. Below this threshold, the particles were considered as false-positive. For each sample, two independent dilutions in filtered PBS were performed and analyzed 5 times.

2.9.2. *In vitro* bioactivity assay of EV: impact on H9c2 cells viability

H9c2 rat cardiac myoblasts were seeded at 25,000 cells/cm² on 0.2% gelatin-coated plates. The medium used was DMEM + glutamax supplemented with 10% (v/v) FBS and 1% (v/v) PSA at 37°C and 5% CO_2. After 24h (corresponding to T0), the H9c2 medium was replaced by a fresh volume of serum-free DMEM loaded with EV at different concentrations to determine their impact on cell viability. The number of cells was determined after 27h-incubation using the cell counting Muse™ (0500-3115, Merck Millipore, Guyancourt, France) coupled with a viability kit (MCH100102, Merck Millipore). Serum-containing and serum-free DMEM were used as positive and negative controls, respectively. The number of cells was normalized against the cell number in serum-free DMEM. Each condition was evaluated in biological duplicates or triplicates and the experiments were performed at least 2 times.

2.9.3. Cryogenic electron microscopy (cryoTEM)

EV solution (2 µL) was deposited on the carbon grid and flash frozen in liquid ethane. The carbon grid was mounted on a holder and directly observed at -180°C using a transmitted

electron microscope (JEOL 2100HC at 200 kV with LaB6 filament). The image acquisition was carried out using the software Digital Micrograph (version 1.83.842, Gatan Inc.).

2.9.4. microRNA analysis

The microRNA (miR) were isolated from EV by following the supplier instructions of the Ambion mirVana miRNA Isolation Kit using a glass fiber filter (GFF)-based method. The miR concentration was evaluated by Bioanalyzer RNA analysis at the genomic platform of hôpital Cochin. The following conditions were tested: non-freeze dried EV, freeze-dried EV and freeze-dried EV resuspended in filtered water and incubated for 5 days at 37°C in aseptic conditions.

2.9.5. Scanning Electron Microscopy

A disc from the different PGSA-g-EG/EV formulations was frozen in OCT medium and subsequently cut into transversal slices (30 µm). The sections were observed using scanning electron microscopy (SEM, JEOL JCM-6000Plus at 10kV, BED-S / PC-std modes).

2.10. Statistical analysis

All data were calculated as mean ± standard deviation, with N as number of experiments and n as number of biological replicates performed. Statistical analysis was carried out using Prism 8.0 (GraphPad, La Jolla, California, USA). The data normality was first analyzed using a Shapiro-Wilk test. If the data passed the normality test, they were compared using two-way analysis of variance (ANOVA) and Tukey post-test (95% CI confidence interval). If the data did not pass the normality test, they were compared using Kruskal-Wallis test + Dunn's post-test. Differences of $p < 0.05$ were considered significant.

3. Results

3.1. PGSA-g-EG extract: *In vitro* cytotoxicity and impact on EV bioactivity

We started by evaluating the impact of PGSA-g-EG extracts on H9c2 rat cardiac myoblast cell number by counting the number of cells after exposure to the polymer extract (Fig. 1A). When incubated in DMEM with 10% FBS, H9c2 cells increased in number by 3.1±0.9-fold

(positive control) when compared to FBS-deprived cells (normalized at 1-fold). After incubation with 1 % (v/v) of PGSA-g-EG extracts in DMEM10%FBS, H9c2 cells increased in number by 3.2±0.9-fold. This dilution was selected to minimize the ratio of PBS to DMEM that could impact the assessment of EV bioactivity in the following experiments. At this concentration, PGSA-g-EG extracts do not induce a negative or positive effect on the cells and such a dilution was therefore deemed to be appropriate for the assessment of EV bioactivity.

We next assessed whether the combination of PGSA-g-EG extracts with EV would affect the capacity of the latter to improve the viability of serum-deprived H9c2 rat cells (Fig. 1B). During the incubation period in DMEM 10%FBS, H9c2 cells proliferated by 2.6±0.5-fold. As previously described [27], EV increased cell viability by 2.2±0.2-fold in serum-deprived conditions. Importantly, a similar viability rate (2.1±0.2-fold increase) was observed in the presence of EV and PGSA-g-EG extracts. In comparison, in serum-deprived DMEM supplemented with PGSA-g-EG extracts alone (PBS-PGSA-g-EG condition), the number of cells changed by 0.8±0.2 fold. These data suggest that PGSA-g-EG extracts do not impact EV bioactivity.

3.2. Biocompatibility of PGSA-g-EG in the rat heart

The PGSA-g-EG polymer biocompatibility on cardiac tissue was assessed (Fig. 2). The polymer was light activated *in situ* and animals were kept alive for one month. This time point was chosen so that the local tissue response to the material could be evaluated with minimal impact from the surgical procedure. Importantly, for all animals, the patch remained at its implantation site during the follow-up period; the adhesion was thus considered adequate for the use of the material as a cardiac patch for delivery of a biologics for at least 1 month.

Histological analysis of the samples revealed the presence of the polymer at the surface of the heart. Minimal/slight (Grade 1/2) inflammatory infiltrates with the presence of mononuclear cells (macrophages) were observed. The Masson's Trichrome staining showed minimal/slight (Grade 1/Grade 2) fibrosis around the polymer disk. No morphologic

alterations were observed in the pericardium or myocardium. The control animals showed no inflammatory infiltrates or fibrosis. These results demonstrate that PGSA-g-EG had no harmful effects on the rat cardiac tissue.

3.3. *In vitro* bioactivity of FD EV and TRE for release formulations

To maximize the loading and stability of EV in the PGSA-g-EG cardiac patch, we evaluated the possibility of obtaining a solid pellet of EV through freeze drying (Fig. 3).

The *in vitro* bioactivity of freeze-dried extracellular vesicles (FD EV) was compared to the bioactivity of non-freeze-dried EV (non-FD EV). When incubated in DMEM 10%FBS the number of cells increased by 2.4±0.2-fold (positive control). Likewise, when incubated in serum-deprived DMEM containing EV, the number of cells increased by 2.2±0.3 when normalized to the negative control ($p<0.05$ vs. serum-deprived DMEM). In serum-deprived DMEM supplemented with FD EV, cell number increased in a similar proportion (2.1±0.3-fold increase), as shown in Fig. 3, thereby suggesting that freeze-drying does not affect the EV bioactivity.

The impact of using trehalose (TRE), a known cryoprotectant and osmotic agent [41–43], as an excipient during EV freeze-drying, was also evaluated. Briefly, when incubated in the presence of EV with 10% TRE or FD EV with 10% TRE, the number of cells increased by 2.1±0.2 and 1.9±0.1, respectively ($p<0.05$ vs. DMEM) (Fig. 3). Similar results were obtained when using 20% of TRE. These data suggest TRE does not impact EV bioactivity.

3.4. EV stability in PBS at 37ºC

During *in vitro* release studies, the EV are released from the PGSA-g-EG polymeric matrix into the aqueous medium (PBS) at 37°C. We therefore evaluated the stability and bioactivity of FD EV under these conditions.

The bioactivity of FD EV incubated in PBS for different time points was evaluated (Fig. 4A). In the presence of DMEM 10% FBS, the number of cell number increased 3.3±0.2 fold (positive control) and this increase was 2.2±0.3 fold in the presence of DMEM with FD EV (EV day0). After 3 days of FD EV incubation in PBS at 37ºC, there was no significant loss

(<10%) of EV bioactivity. However, when the FD EV were incubated for 9 days, cell number only increased by 1.8±0.2 fold. A steady decrease in bioactivity was observed for later time points. After 60 days of incubation, 40% bioactivity of the FD EV bioactivity was lost when compared to day 0 ($p<0.05$ vs EV day0). Similarly, the bioactivity of FD EV in the presence of 2.5% TRE (FD EV/2.5% TRE) decreased during incubation (Fig. 4B). Overall, these data indicate that EV feature a time-dependent loss of their bioactivity when incubated at 37°C in PBS.

To investigate the root cause of bioactivity loss, the non-FD and FD EV were characterized by cryo-transmitted electron microscopy and miR quantification at 0 and 5 days of incubation at 37°C in PBS. Cryo-techniques were selected since no sample fixation is required and the membrane integrity is maintained [44].

Prior to incubation, the diameter of FD and non-FD EV was between 30nm and 800nm. The EV formed relatively small aggregates with a maximal diameter of 1 to 1.5µm and with up to 25 distinct vesicles. Multivesicular EV were observed, but these were limited to less than 5 merged vesicles. No qualitative difference between non-FD (Fig. 5A) and FD (Fig. 5B) EV were observed. Similar observations were made in the presence of 2.5% TRE (Figs. 5D and 5E).

After 5 days of incubation in PBS at 37°C, the FD EV (with or without TRE) tended to form larger aggregates that could reach 4 µm in diameter and included hundreds of vesicles. Moreover, fusion of vesicles was observed. Multilamellar aggregates with about ten contiguous membranes were observed (Figs. 5C and 5F).

Quantification of miRNA was conducted for both FD and non-FD EV at 0 and 5 days of incubation in PBS at 37°C (Fig. 6). The concentration of miR in EV was 568±187 µg/µL and did not differ in freeze-dried EV (572±216 µg/µL, $p=0.68$ vs. EV). For the EV/2.5%TRE, the miR concentration before and after freeze-drying reached 361±88 µg/µL and 419±82 µg/µL,

respectively (p=0.70) (Fig 6). Thus, no significant differences in miR concentration were observed after freeze-drying for both formulations.

However, after 5 days of incubation in PBS at 37ºC, the miR concentration of EV decreased to 103±5 µg/µL while for EV/2.5%TRE, it was 108±46 µg/µL. This corresponded to a decrease of more than 70% in miR concentrations, confirming the detrimental impact of prolonged incubation on EV structure and content, independently of the presence of TRE.

3.5. Preparation of PGSA-g-EG and EV formulations

Grinded FD EV and FD EV/2.5% TRE were manually mixed with PGSA-g-EG, followed by light activation. Cross-sections of the polymerized material were observed using scanning electron microscopy (Fig. 7). No qualitative differences could be observed between both formulations.

3.6. Release of EV from PGSA-g-EG formulations.

The *in vitro* bioactivity of different EV doses was evaluated on serum-deprived H9c2 cells (Fig. 8A). As previously described [27], the bioactivity of EV on H9c2 cells is concentration-dependent. This effect was reproducible for different EV formulations and independently of the presence of TRE. The dose effect could be mathematically represented by a second-degree polynomial. This dose-bioactivity correlation was used as a calibration curve to determine the release kinetics for the different PGSA-g-EG formulations.

Bioactive FD EV could be released from the PGSA-g-EG polymer for up to 5 days (Figs. 8A and C), as demonstrated by the increased cell number when compared to the negative control, ($p<0.05$ vs. serum deprived DMEM). However, no bioactive EV were detected at later time points.

Similarly, the bioactivity of FD EV/2.5% TRE released from the PGSA-g-EG polymer was evaluated over time (Figs. 8B and 8D). For this formulation, bioactive EV could be released up to 14 days. At this time point the H9c2 cells exposed to EV still increased their count by 1.7±0.2 fold ($p<0.05$ vs serum-deprived DMEM). Beyond this time point, no bioactive EV

were detected. Overall, the presence of TRE enabled to tune the release profile and extend the duration of release of bioactive EV.

4. Discussion

It has been previously shown that repeated injections of EV maximize their therapeutic outcome [31,32]. However, when a local cardiac delivery is privileged, the invasiveness of the approach precludes to repeat it. One possible way of tackling this challenge would be to use an EV delivery vehicle enabling their sustained release. Thus, this study aimed to establish a proof of concept for the controlled release of EV from an adhesive PGSA-g-EG polymer.

We first demonstrated that the PGSA-g-EG extract is not detrimental to cells and does not compromise EV bioactivity either (Fig. 1). *In vitro*, PGSA-g-EG extracts did not impact EV bioactivity on H9c2 cells under serum-deprived conditions. *In vivo* data confirmed the biocompatibility of PGSA-g-EG (Fig. 2). The uncured polymer could be easily applied to the rat left ventricle and did not drip to the surrounding tissue due to its viscous nature, as previously described [37]. Once in the targeted location, it was cured on demand using a LED light [40]. The patch remained adhesive on the heart for at least one month and generated a very mild local tissue response (Fig. 2).

Considering previous studies in mice [27] and the quantity of EV used for epicardial EV delivery using biomaterials [34,35], it was extrapolated that around $4.5x10^{10}$ of EV should be delivered to the heart for inducing a therapeutic benefit in the rat model of post-MI left ventricular dysfunction. A freeze-drying method was therefore developed to formulate EV in a solid form and increase their total loading into PGSA-g-EG. Freeze-drying is widely used to preserve thermosensitive biological materials such as proteins, peptides, liposomes or even EV [45]. To protect the EV and their cargo from the potential detrimental impact of freezing and desiccation steps, the use of cryoprotective agents (CPA) has been described [46]. The most commonly used CPA are disaccharides such as glucose, lactose, sucrose and

trehalose (TRE). TRE can also promote peptide/protein stabilization, suppress surface adsorption, facilitate EV dispersion into formulations and provide physiological osmolality [42]. TRE has been described as the most effective disaccharide to preserve EV or liposomes during freeze-drying [43,47,48] by preventing aggregation and cryodamage [43]. Furthermore, this excipient is widely used in FDA-approved pharmaceutical formulations [41,49]. However, the effect of these CPA on the EV used in this study remained to be demonstrated.

Our results show that freeze-dried EV, with or without TRE, have the same bioactivity than their non-freeze-dried counterparts (Fig. 3). Upon freeze-drying, the EV did not aggregate or fuse (Fig. 5) and no decrease in miR concentration was observed (Fig. 6). Therefore, iPS-Pg-derived EV may not require excipients to preserve their bioactivity upon freeze-drying. In contrast, a recent study showed that TRE was necessary to protect EV secreted by murine MIN6 β-cells during freeze-drying [43]. The stability of the EV may vary with the cell origin, the isolation methods, surface proteins and fatty acid composition and nature of the cargo. This hypothesis is reinforced by studies on liposome stability showing that surface composition has a critical role [50].

The stability of freeze-dried EV or freeze-dried EV/2.5% TRE was then evaluated in PBS at 37°C (Fig. 4) to determine whether it could impact the *in vitro* bioactivity assessment of released EV. A steady decrease in bioactivity was observed as a function of the incubation time (Fig. 4), which could be due to EV aggregation and fusion, as assessed by cryo-transmitted electron microscopy (Fig. 5), and decrease in the miR content (Fig. 6). However, this delayed loss of bioactivity likely reflects the shielding effects of PGSA-g-EG whose hydrophobic properties may protect the EV from aqueous degradation. The lack of proportional correlation between the miR concentration decay and loss of bioactivity may be explained by the fact that miR are not the only factors responsible for EV bioactivity [51].

Quantification of the release of EV from the cured PGSA-g-EG formulations could not rely on NTA because of the confounding effect of polymer extracts [52]. However, a recent study has

demonstrated that the viability effect of cardiac progenitor-derived EV is dose-dependent [27]. This correlation was used to quantify the release of EV from PGSA-g-EG formulations (Figs. 8A and 8B), with the caveat that the bioactivity loss in the aqueous release medium at 37ºC is not taken into consideration. Despite this limitation, it is noteworthy that whereas the EV release after 5 days was limited to 38% in the absence of TRE, 70% of TRE-containing EV (~ $4.2x10^{10}$ EV) were released after 14 days. For conditions with TRE as an excipient, the released loading was higher than for conditions with EV alone. This suggests that the osmotic effect [41] of TRE can be used to control the EV release kinetics.

In two recent studies, the release of EV derived from iPSC-derived cardiomyocytes [34] and endothelial progenitor cells [35] from two different hydrogels was evaluated *in vitro.* $3x10^{10}$ EV were loaded into a 100-mg collagen patch and fully released *in vitro* in 21 days [34]. In another study, approximately $2x10^{10}$ particles were released over 21 days from a hyaluronic acid patch. The patch size and EV loading percentage were not reported [35]. In comparison, with 28% of loading into PGSA-g-EG, the loading of EV/2.5%TRE represented an amount of $6.2x10^{10}$ EV for a patch of 70 mg with a release of approximately $4.2x10^{10}$ of bioactive EV in 14 days.

Thus, with a suitable formulation of EV, a polymer like PGSA-g-EG may be an appropriate delivery vector for their controlled release. This has been demonstrated by the capacity of the polymer to release EV over several days while its release kinetics could be further fine-tuned through changes in its network, such as the degree of crosslinking.

This study provides a first assessment of the potential of PGSA-g-EG to be used as a vehicle to deliver EV in a controlled manner as well as its capacity to adhere to the heart tissue with good biocompatibility after 1 month of implantation. Because of the use of a healthy animal model, no functional testing of the impact on cardiac function was yet performed. Another limitation of the study is the use of the bioactivity assay to quantify EV released from the polymeric matrix. While we could demonstrate that the impact on EV on H9c2 cell count is concentration-dependent, other characterization methods could be used to validate such

results and provide a more accurate quantification. Of note, in the course of this study, we have attempted to develop several of these quantification methods, such as Nanoparticle Tracking Analysis, image flow cytometry and CD63 ELISA assays, but they did not provide reliable results due to interference from polymer residues and insufficient detection limits. It is also important to note that for some of the experiments, a small number of replicates were performed and future studies are required to further validate the current data set. Another consideration is that a range of EV sizes were loaded in the PGSA-g-EG patch. There is currently a lack of consensus regarding the sub-population endowed with the greatest cardioprotective effect and the selective isolation of EV sub-populations remains challenging. Admittedly, the choice of a specific sub-population could modify the EV stability, their release kinetics and the overall bioactivity of the patch.

The development of the technology described in the manuscript may provide significant advantages for the translation of EV as a therapy of heart failure, since it would potentially avoid the requirement of repeated dose administrations while maximizing the therapeutic benefit of EV by guaranteeing a controlled and sustained delivery to the targeted tissue. Furthermore, the use of an adhesive may facilitate its minimally invasive delivery to the targeted tissue.

The biological bioactivity of the released EV from the PGSA-g-EG adhesive polymer remains to be demonstrated *in vivo*. Future work should focus on validating this concept and demonstrating the capacity of PGSA-g-EG to release bioactive EV in a chronic heart failure model. The EV dose and release kinetic requirements to guarantee such a therapeutic benefit will also require further investigations.

5. Conclusion

This study demonstrated *in vitro* that PGSA-g-EG is able to release EV secreted by cardiovascular progenitors differentiated from iPSC. To tune the release kinetics, specific

formulations of freeze-dried EV were developed and shown to be structurally and stably bioactive. Moreover, despite the degradation and the instability of EV in aqueous medium, the PGSA-g-EG polymer was able to release bioactive EV for at least 14 days, which suggests the capability of the PGSA-g-EG to protect EV from aqueous degradation.

Furthermore, in an *in vivo* rat model, the polymer did not induce an inflammatory response and remained adherent to the epicardium for at least one month, thereby demonstrating the potential of the material to be used for targeted and local delivery of bioactive agents.

Further work should now assess the therapeutic effect of the released EV in preclinical models of post-MI left ventricular dysfunction.

6. Disclosure.

MJNP is an employee and holds stock options in Tissium, a company that further licensed IP generated by MJNP and that may benefit financially if the IP is further validated. MJNP has filed patents based on materials described in this manuscript.

7. Funding

This work was supported by the Institut National de la Santé et de la Recherche Médicale (Inserm), the Agence Nationale de la Recherche (EXOGEL program ANR-17-CE18-0003) and Tissium S.A.

8. References

[1] P. Ponikowski, A.A. Voors, S.D. Anker, H. Bueno, J.G.F. Cleland, A.J.S. Coats, V. Falk, J.R. González-Juanatey, V.-P. Harjola, E.A. Jankowska, M. Jessup, C. Linde, P. Nihoyannopoulos, J.T. Parissis, B. Pieske, J.P. Riley, G.M.C. Rosano, L.M. Ruilope, F. Ruschitzka, F.H. Rutten, P. van der Meer, ESC Scientific Document Group, 2016 ESC Guidelines for the diagnosis and treatment of acute and chronic heart failure, Eur. Heart J. 37 (2016) 2129–2200. https://doi.org/10.1093/eurheartj/ehw128.

[2] V.L. Roger, Epidemiology of Heart Failure, Circ. Res. 113 (2013) 646–659. https://doi.org/10.1161/CIRCRESAHA.113.300268.

[3] O. Bergmann, R.D. Bhardwaj, S. Bernard, S. Zdunek, F. Barnabé-Heider, S. Walsh, J. Zupicich, K. Alkass, B.A. Buchholz, H. Druid, S. Jovinge, J. Frisén, Evidence for Cardiomyocyte Renewal in Humans, Science (80-.). 324 (2009) 98–102. https://doi.org/10.1126/SCIENCE.1164680.

[4] K. Thygesen, J.S. Alpert, A.S. Jaffe, M.L. Simoons, B.R. Chaitman, H.D. White, K. Thygesen, J.S. Alpert, H.D. White, A.S. Jaffe, H.A. Katus, F.S. Apple, B. Lindahl, D.A. Morrow, B.R. Chaitman, P.M. Clemmensen, P. Johanson, H. Hod, R. Underwood, J.J. Bax, R.O. Bonow, F. Pinto, R.J. Gibbons, K.A. Fox, D. Atar, L.K. Newby, M. Galvani, C.W. Hamm, B.F. Uretsky, P. Gabriel Steg, W. Wijns, J.-P. Bassand, P. Menasché, J. Ravkilde, E.M. Ohman, E.M. Antman, L.C. Wallentin, P.W. Armstrong, M.L. Simoons, J.L. Januzzi, M.S. Nieminen, M. Gheorghiade, G. Filippatos, R. V. Luepker, S.P. Fortmann, W.D. Rosamond, D. Levy, D. Wood, S.C. Smith, D. Hu, J.-L. Lopez-Sendon, R.M. Robertson, D. Weaver, M. Tendera, A.A. Bove, A.N. Parkhomenko, E.J. Vasilieva, S. Mendis, J.J. Bax, H. Baumgartner, C. Ceconi, V. Dean, C. Deaton, R. Fagard, C. Funck-Brentano, D. Hasdai, A. Hoes, P. Kirchhof, J. Knuuti, P. Kolh, T. McDonagh, C. Moulin, B.A. Popescu, Ž. Reiner, U. Sechtem, P.A. Sirnes, M. Tendera, A. Torbicki, A. Vahanian, S. Windecker, J. Morais, C. Aguiar, W. Almahmeed, D.O.

Arnar, F. Barili, K.D. Bloch, A.F. Bolger, H.E. Bøtker, B. Bozkurt, R. Bugiardini, C. Cannon, J. de Lemos, F.R. Eberli, E. Escobar, M. Hlatky, S. James, K.B. Kern, D.J. Moliterno, C. Mueller, A.N. Neskovic, B.M. Pieske, S.P. Schulman, R.F. Storey, K.A. Taubert, P. Vranckx, D.R. Wagner, Third universal definition of myocardial infarction, Eur. Heart J. 33 (2012) 2551–2567. https://doi.org/10.1093/eurheartj/ehs184.

[5] M. Jessup, S. Brozena, Heart Failure, N. Engl. J. Med. 348 (2003) 2007–2018. https://doi.org/10.1056/NEJMra021498.

[6] V.F.M. Segers, R.T. Lee, Stem-cell therapy for cardiac disease, Nature. 451 (2008) 937–942. https://doi.org/10.1038/nature06800.

[7] P. Müller, H. Lemcke, R. David, Stem Cell Therapy in Heart Diseases – Cell Types, Mechanisms and Improvement Strategies, Cell. Physiol. Biochem. 48 (2018) 2607–2655. https://doi.org/10.1159/000492704.

[8] N.H. Goradel, F.G.- Hour, B. Negahdari, Z.V. Malekshahi, M. Hashemzehi, A. Masoudifar, H. Mirzaei, Stem Cell Therapy: A New Therapeutic Option for Cardiovascular Diseases, J. Cell. Biochem. 119 (2018) 95–104. https://doi.org/10.1002/jcb.26169.

[9] V. Karantalis, J.M. Hare, Use of Mesenchymal Stem Cells for Therapy of Cardiac Disease, Circ. Res. 116 (2015) 1413–1430. https://doi.org/10.1161/CIRCRESAHA.116.303614.

[10] V.F.M. Segers, R.T. Lee, Stem-cell therapy for cardiac disease, Nature. 451 (2008) 937–942. https://doi.org/10.1038/nature06800.

[11] M.F. Pittenger, B.J. Martin, Mesenchymal stem cells and their potential as cardiac therapeutics., Circ. Res. 95 (2004) 9–20. https://doi.org/10.1161/01.RES.0000135902.99383.6f.

[12] C.E. Murry, M.H. Soonpaa, H. Reinecke, H. Nakajima, H.O. Nakajima, M. Rubart,

K.B.S. Pasumarthi, J. Ismail Virag, S.H. Bartelmez, V. Poppa, G. Bradford, J.D. Dowell, D.A. Williams, L.J. Field, Haematopoietic stem cells do not transdifferentiate into cardiac myocytes in myocardial infarcts, Nature. 428 (2004) 664–668. https://doi.org/10.1038/nature02446.

[13] J.M. Karp, G.S. Leng Teo, Mesenchymal Stem Cell Homing: The Devil Is in the Details, Cell Stem Cell. 4 (2009) 206–216. https://doi.org/10.1016/J.STEM.2009.02.001.

[14] L. Timmers, S.K. Lim, F. Arslan, J.S. Armstrong, I.E. Hoefer, P.A. Doevendans, J.J. Piek, R.M. El Oakley, A. Choo, C.N. Lee, G. Pasterkamp, D.P.V. de Kleijn, Reduction of myocardial infarct size by human mesenchymal stem cell conditioned medium, Stem Cell Res. 1 (2008) 129–137. https://doi.org/10.1016/j.scr.2008.02.002.

[15] L. Timmers, S.K. Lim, I.E. Hoefer, F. Arslan, R.C. Lai, A.A.M. van Oorschot, M.J. Goumans, C. Strijder, S.K. Sze, A. Choo, J.J. Piek, P.A. Doevendans, G. Pasterkamp, D.P.V. de Kleijn, Human mesenchymal stem cell-conditioned medium improves cardiac function following myocardial infarction, Stem Cell Res. 6 (2011) 206–214. https://doi.org/10.1016/J.SCR.2011.01.001.

[16] R. Kishore, M. Khan, More Than Tiny Sacks: Stem Cell Exosomes as Cell-Free Modality for Cardiac Repair., Circ. Res. 118 (2016) 330–43. https://doi.org/10.1161/CIRCRESAHA.115.307654.

[17] G. van Niel, G. D'Angelo, G. Raposo, Shedding light on the cell biology of extracellular vesicles, Nat. Rev. Mol. Cell Biol. 19 (2018) 213–228. https://doi.org/10.1038/nrm.2017.125.

[18] S.L.N. Maas, X.O. Breakefield, A.M. Weaver, Extracellular Vesicles: Unique Intercellular Delivery Vehicles., Trends Cell Biol. 27 (2017) 172–188. https://doi.org/10.1016/j.tcb.2016.11.003.

[19] M. Colombo, G. Raposo, C. Théry, Biogenesis, Secretion, and Intercellular Interactions of Exosomes and Other Extracellular Vesicles, Annu. Rev. Cell Dev. Biol. 30 (2014) 255–289. https://doi.org/10.1146/annurev-cellbio-101512-122326.

[20] J.C. Akers, D. Gonda, R. Kim, B.S. Carter, C.C. Chen, Biogenesis of extracellular vesicles (EV): exosomes, microvesicles, retrovirus-like vesicles, and apoptotic bodies, J. Neurooncol. 113 (2013) 1–11. https://doi.org/10.1007/s11060-013-1084-8.

[21] S. Sahoo, D.W. Losordo, Exosomes and Cardiac Repair After Myocardial Infarction, Circ. Res. 114 (2014) 333–344. https://doi.org/10.1161/CIRCRESAHA.114.300639.

[22] M. Khan, E. Nickoloff, T. Abramova, J. Johnson, S.K. Verma, P. Krishnamurthy, A.R. Mackie, E. Vaughan, V.N.S. Garikipati, C. Benedict, V. Ramirez, E. Lambers, A. Ito, E. Gao, S. Misener, T. Luongo, J. Elrod, G. Qin, S.R. Houser, W.J. Koch, R. Kishore, Embryonic Stem Cell-Derived Exosomes Promote Endogenous Repair Mechanisms and Enhance Cardiac Function Following Myocardial Infarction, Circ. Res. 117 (2015) 52–64. https://doi.org/10.1161/CIRCRESAHA.117.305990.

[23] L. Huang, W. Ma, Y. Ma, D. Feng, H. Chen, B. Cai, Exosomes in mesenchymal stem cells, a new therapeutic strategy for cardiovascular diseases?, Int. J. Biol. Sci. 11 (2015) 238–45. https://doi.org/10.7150/ijbs.10725.

[24] C. Merino-González, F.A. Zuñiga, C. Escudero, V. Ormazabal, C. Reyes, E. Nova-Lamperti, C. Salomón, C. Aguayo, Mesenchymal Stem Cell-Derived Extracellular Vesicles Promote Angiogenesis: Potencial Clinical Application, Front. Physiol. 7 (2016). https://doi.org/10.3389/FPHYS.2016.00024.

[25] R.C. Lai, F. Arslan, M.M. Lee, N.S.K. Sze, A. Choo, T.S. Chen, M. Salto-Tellez, L. Timmers, C.N. Lee, R.M. El Oakley, G. Pasterkamp, D.P.V. de Kleijn, S.K. Lim, Exosome secreted by MSC reduces myocardial ischemia/reperfusion injury, Stem Cell Res. 4 (2010) 214–222. https://doi.org/10.1016/j.scr.2009.12.003.

[26] A. Kervadec, V. Bellamy, N. El Harane, L. Arakélian, V. Vanneaux, I. Cacciapuoti, H. Nemetalla, M.-C. Périer, H.D. Toeg, A. Richart, M. Lemitre, M. Yin, X. Loyer, J. Larghero, A. Hagège, M. Ruel, C.M. Boulanger, J.-S. Silvestre, P. Menasché, N.K.E. Renault, Cardiovascular progenitor–derived extracellular vesicles recapitulate the beneficial effects of their parent cells in the treatment of chronic heart failure, J. Hear. Lung Transplant. 35 (2016) 795–807. https://doi.org/10.1016/j.healun.2016.01.013.

[27] N. El Harane, A. Kervadec, V. Bellamy, L. Pidial, H.J. Neametalla, M.C. Perier, B. Lima Correa, L. Thiébault, N. Cagnard, A. Duché, C. Brunaud, M. Lemitre, J. Gauthier, A.T. Bourdillon, M.P. Renault, Y. Hovhannisyan, S. Paiva, A.R. Colas, O. Agbulut, A. Hagège, J.S. Silvestre, P. Menasché, N.K.E. Renault, Acellular therapeutic approach for heart failure: In vitro production of extracellular vesicles from human cardiovascular progenitors, Eur. Heart J. 39 (2018) 1835–1847. https://doi.org/10.1093/eurheartj/ehy012.

[28] L. Barile, V. Lionetti, E. Cervio, M. Matteucci, M. Gherghiceanu, L.M. Popescu, T. Torre, F. Siclari, T. Moccetti, G. Vassalli, Extracellular vesicles from human cardiac progenitor cells inhibit cardiomyocyte apoptosis and improve cardiac function after myocardial infarction, Cardiovasc. Res. 103 (2014) 530–541. https://doi.org/10.1093/cvr/cvu167.

[29] F.G. Thankam, D.K. Agrawal, Infarct Zone: a Novel Platform for Exosome Trade in Cardiac Tissue Regeneration, J. Cardiovasc. Transl. Res. (2020). https://doi.org/10.1007/s12265-019-09952-8.

[30] M. Adamiak, S. Sahoo, Exosomes in Myocardial Repair: Advances and Challenges in the Development of Next-Generation Therapeutics., Mol. Ther. 26 (2018) 1635–1643. https://doi.org/10.1016/j.ymthe.2018.04.024.

[31] S. Zhang, W.C. Chu, R.C. Lai, S.K. Lim, J.H.P. Hui, W.S. Toh, Exosomes derived from human embryonic mesenchymal stem cells promote osteochondral regeneration,

Osteoarthr. Cartil. 24 (2016) 2135–2140. https://doi.org/10.1016/j.joca.2016.06.022.

[32] X. Liu, Y. Yang, Y. Li, X. Niu, B. Zhao, Y. Wang, C. Bao, Z. Xie, Q. Lin, L. Zhu, Integration of stem cell-derived exosomes with in situ hydrogel glue as a promising tissue patch for articular cartilage regeneration, Nanoscale. 9 (2017) 4430–4438. https://doi.org/10.1039/C7NR00352H.

[33] M.J.N. Pereira, I.F. Carvalho, J.M. Karp, L.S. Ferreira, Sensing the Cardiac Environment: Exploiting Cues for Regeneration, J. Cardiovasc. Transl. Res. 4 (2011) 616–630. https://doi.org/10.1007/s12265-011-9299-6.

[34] B. Liu, B.W. Lee, K. Nakanishi, A. Villasante, R. Williamson, J. Metz, J. Kim, M. Kanai, L. Bi, K. Brown, G. Di Paolo, S. Homma, P.A. Sims, V.K. Topkara, G. Vunjak-Novakovic, Cardiac recovery via extended cell-free delivery of extracellular vesicles secreted by cardiomyocytes derived from induced pluripotent stem cells., Nat. Biomed. Eng. 2 (2018) 293–303. https://doi.org/10.1038/s41551-018-0229-7.

[35] C.W. Chen, L.L. Wang, S. Zaman, J. Gordon, M.F. Arisi, C.M. Venkataraman, J.J. Chung, G. Hung, A.C. Gaffey, L.A. Spruce, H. Fazelinia, R.C. Gorman, S.H. Seeholzer, J.A. Burdick, P. Atluri, Sustained release of endothelial progenitor cell-derived extracellular vesicles from shear-thinning hydrogels improves angiogenesis and promotes function after myocardial infarction, Cardiovasc. Res. 114 (2018) 1029–1040. https://doi.org/10.1093/cvr/cvy067.

[36] ‡ Christiaan L. E. Nijst, †, † Joost P. Bruggeman, ‖ Jeffrey M. Karp, † Lino Ferreira, † Andreas Zumbuehl, † and Christopher J. Bettinger, † Robert Langer*, Synthesis and Characterization of Photocurable Elastomers from Poly(glycerol-co-sebacate), (2007). https://doi.org/10.1021/BM070423U.

[37] N. Lang, M.J. Pereira, Y. Lee, I. Friehs, N. V Vasilyev, E.N. Feins, K. Ablasser, E.D. O'Cearbhaill, C. Xu, A. Fabozzo, R. Padera, S. Wasserman, F. Freudenthal, L.S. Ferreira, R. Langer, J.M. Karp, P.J. del Nido, A blood-resistant surgical glue for

minimally invasive repair of vessels and heart defects., Sci. Transl. Med. 6 (2014) 218ra6. https://doi.org/10.1126/scitranslmed.3006557.

[38] A. Mahdavi, L. Ferreira, C. Sundback, J.W. Nichol, E.P. Chan, D.J.D. Carter, C.J. Bettinger, S. Patanavanich, L. Chignozha, E. Ben-Joseph, A. Galakatos, H. Pryor, I. Pomerantseva, P.T. Masiakos, W. Faquin, A. Zumbuehl, S. Hong, J. Borenstein, J. Vacanti, R. Langer, J.M. Karp, A biodegradable and biocompatible gecko-inspired tissue adhesive, Proc. Natl. Acad. Sci. 105 (2008) 2307–2312. https://doi.org/10.1073/pnas.0712117105.

[39] S. Gerecht, S.A. Townsend, H. Pressler, H. Zhu, C.L.E. Nijst, J.P. Bruggeman, J.W. Nichol, R. Langer, A porous photocurable elastomer for cell encapsulation and culture, Biomaterials. 28 (2007) 4826–4835. https://doi.org/10.1016/J.BIOMATERIALS.2007.07.039.

[40] Q. Pellenc, J. Touma, R. Coscas, G. Edorh, M. Pereira, J. Karp, Y. Castier, P. Desgranges, J.M. Alsac, Preclinical and clinical evaluation of a novel synthetic bioresorbable, on demand light activated sealant in vascular reconstruction., J. Cardiovasc. Surg. (Torino). (2019). https://doi.org/10.23736/S0021-9509.19.10783-5.

[41] S. Ohtake, Y.J. Wang, Trehalose: Current Use and Future Applications, J. Pharm. Sci. 100 (2011) 2020–2053. https://doi.org/10.1002/jps.22458.

[42] C. Olsson, H. Jansson, J. Swenson, The Role of Trehalose for the Stabilization of Proteins, J. Phys. Chem. B. 120 (2016) 4723–4731. https://doi.org/10.1021/acs.jpcb.6b02517.

[43] S. Bosch, L. de Beaurepaire, M. Allard, M. Mosser, C. Heichette, D. Chrétien, D. Jegou, J.-M. Bach, Trehalose prevents aggregation of exosomes and cryodamage, Sci. Rep. 6 (2016) 36162. https://doi.org/10.1038/srep36162.

[44] K.W. Witwer, E.I. Buzás, L.T. Bemis, A. Bora, C. Lässer, J. Lötvall, E.N. Nolte-'t Hoen,

M.G. Piper, S. Sivaraman, J. Skog, C. Théry, M.H. Wauben, F. Hochberg, Standardization of sample collection, isolation and analysis methods in extracellular vesicle research, J. Extracell. Vesicles. 2 (2013) 20360. https://doi.org/10.3402/jev.v2i0.20360.

[45] G.D. Kusuma, M. Barabadi, J.L. Tan, D.A. V. Morton, J.E. Frith, R. Lim, To Protect and to Preserve: Novel Preservation Strategies for Extracellular Vesicles, Front. Pharmacol. 9 (2018) 1199. https://doi.org/10.3389/fphar.2018.01199.

[46] S. Bhattacharya, Cryopretectants and Their Usage in Cryopreservation Process, in: Cryopreserv. Biotechnol. Biomed. Biol. Sci., IntechOpen, 2018. https://doi.org/10.5772/intechopen.80477.

[47] C. Chen, D. Han, C. Cai, X. Tang, An overview of liposome lyophilization and its future potential, J. Control. Release. 142 (2010) 299–311. https://doi.org/10.1016/j.jconrel.2009.10.024.

[48] M. Kreke, R. Smith, P. HANSCOME, K. PECK, A. Ibrahim, Processes for producing stable exosome formulations, 2014. https://patents.google.com/patent/US20160158291A1/en (accessed June 6, 2019).

[49] J. Corver, P.-J. Van Bockstal, T. De Beer, A continuous and controlled pharmaceutical freeze-drying technology for unit doses, Eur. Pharm. Rev. 22 (2017) 51–53. https://www.europeanpharmaceuticalreview.com/article/70823/continuous-controlled-pharmaceutical-freeze-drying-technology-unit-doses/ (accessed June 6, 2019).

[50] A. Szcześ, M. Jurak, E. Chibowski, Stability of binary model membranes—Prediction of the liposome stability by the Langmuir monolayer study, J. Colloid Interface Sci. 372 (2012) 212–216. https://doi.org/10.1016/J.JCIS.2012.01.035.

[51] E. Lazar, T. Benedek, S. Korodi, N. Rat, J. Lo, I. Benedek, Stem cell-derived exosomes - an emerging tool for myocardial regeneration., World J. Stem Cells. 10

(2018) 106–115. https://doi.org/10.4252/wjsc.v10.i8.106.

[52] C.Y. Soo, Y. Song, Y. Zheng, E.C. Campbell, A.C. Riches, F. Gunn-Moore, S.J. Powis, Nanoparticle tracking analysis monitors microvesicle and exosome secretion from immune cells., Immunology. 136 (2012) 192–7. https://doi.org/10.1111/j.1365-.2567.2012.03569.x.

Figure Legends

Fig 1: PGSA-g-EG shows neither *in vitro* cytotoxicity nor a detrimental impact on EV bioactivity. (A) H9c2 rat cardiac myoblast viability assay after 27-h incubation with 1% (v/v) PGSA-g-EG polymer extract. These extracts did not negatively impact cell viability. Results are the average cell counts of 3 independent experiments (N=3), each in duplicate (n=2). **(B)** EV bioactivity after contact with PGSA-g-EG. The EV bioactivity was not impacted by exposure to the polymer extract. The experiment was performed on two different production batches of PGSA-g-EG. Results are the average of the number of cells measured in 2 independent experiments (N=2), each in duplicate (n=2). *** P <0.0005, **** P <0.0001

Fig 2: *In situ* cured PGSA-g-EG leads to a minimal inflammatory response of the cardiac tissue in a rat model. Representative HES and TM staining of cardiac tissue sections of (**A, B, C**) sham animals (n=3) and (**D, E, F**) animals implanted with PGSA-g-EG (n=3). The red star indicates the location of the implantation of the PGSA-g-EG polymer; the red and green arrows indicate the fibrosis and mononuclear cells around the polymer disk, respectively. (**G**) Quantitative assessment of the microscopic findings by an independent pathologist: NS: Non-Significant; Grade 1: Minimal; Grade 2: Slight; Grade 3: Moderate; Grade 4: Marked; Grade 5: Massive.

Fig 3: EV bioactivity is preserved upon freeze-drying. Non-freeze dried EV (EV) and freeze-dried EV (FD EV) supplemented with 0%, 10%, or 20% (w/v) of TRE supported H9c2 rat cardiac myoblast viability in serum-deprived conditions. Results are the average number of cells measured in 3 independent experiments (N=3), each in duplicate (n=2). * P <0.05

Fig 4: The bioactivity of EV and FD EV decreases over time when incubated in PBS at 37°C. Bioactivity of **(A)** FD EV and **(B)** FD EV/2.5% during the incubation period, measured using the H9c2 cell viability assay. Results are the average cell counts of 2 independent experiments (N=2), each in triplicate (n=3). * P <0.05, ** P <0.005, *** P <0.0005, **** P <0.0001

Fig 5: EV aggregated and fused after 5 days of incubation in PBS at 37°C. Representative cryo-TEM micrographs from **(A)** Non-FD EV, **(B)** FD EV, **(C)** FD EV after 5 days of incubation in PBS at 37°C, **(D)** Non-FD EV / 2.5% TRE, **(E)** FD EV / 2.5% TRE, **(F)** FD EV / 2.5% TRE after 5 days of incubation in PBS at 37°C. Overall, EV showed normal structural features before incubation in PBS; however, after incubation in PBS, aggregation, and fusion of EV were observed.

Fig 6: EV miR concentration is not impacted by freeze-drying but decreases during incubation in PBS at 37°C. miR quantification from EV and EV / 2.5% TRE, before and after freeze-drying, and after 5 days of incubation at 37°C in PBS. Results are the average of a duplicate (n=2)

Fig 7: Scanning Electron Micrograph of PGSA-g-EG disc cross-sections. Discs were formulated with **(A)** FD EV **(B)** FD EV / 2.5% TRE. The arrows indicate the freeze-dried EV formulations. No qualitative difference could be observed between both formulations.

Fig 8: PGSA-g-EG releases bioactive EV for at least 14 days. *In vitro* bioactivity of different concentrations of EV (in green) and released EV (in orange) from **(A)** PGSA-g-EG polymer disc loaded with 19% w/w of FD EV and **(B)** PGSA-g-EG polymer disc loaded with 28% w/w of FD EV / 2.5% TRE. *In vitro* release kinetics of EV from PGSA-g-EG polymer disc with different loadings of **(C)** FD EV and **(D)** FD EV / 2.5% TRE. Results are the average of 2 independent experiments (N=2), each in triplicate (n=3). * P <0.05, ** P <0.005, *** P <0.0005

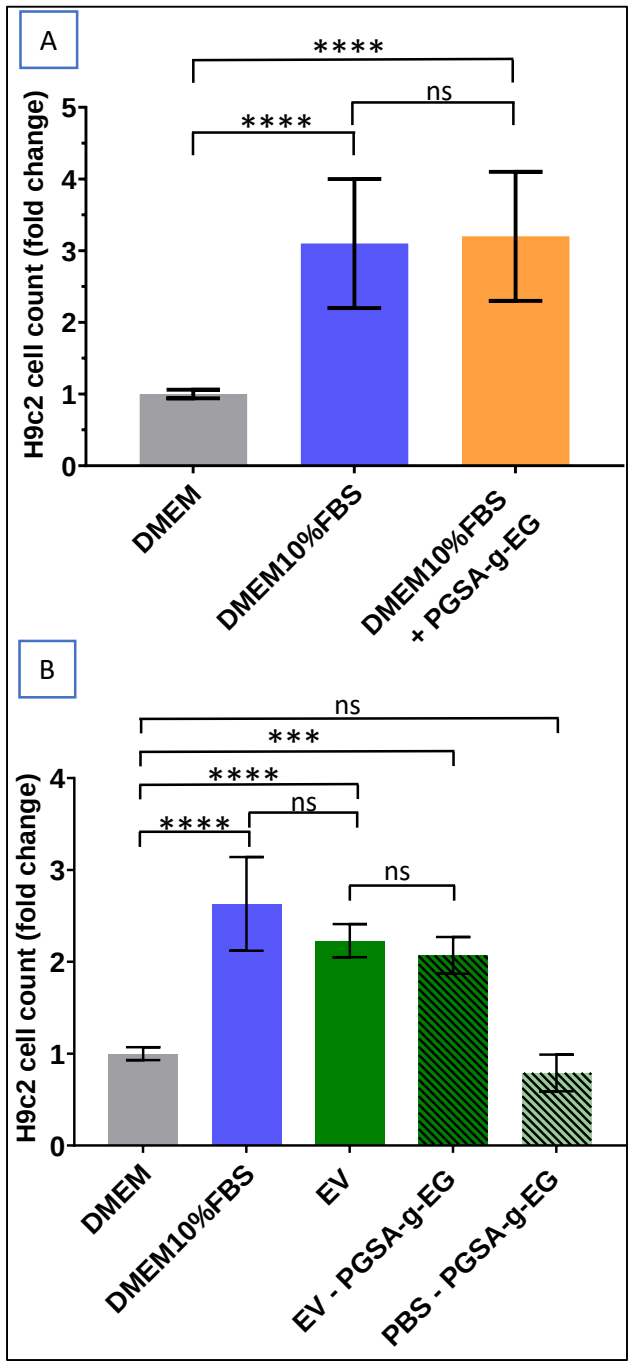
A
****
ns
****
H9c2 cell count (fold change)
5
4
3
2
1
0
DMEM
DMEM10%FBS
DMEM10%FBS
+ PGSA-g-EG
B
ns
***
****
ns
****
ns
H9c2 cell count (fold change)
4
3
2
1
0
DMEM
DMEM10%FBS
EV
EV - PGSA-g-EG
PBS - PGSA-g-EG

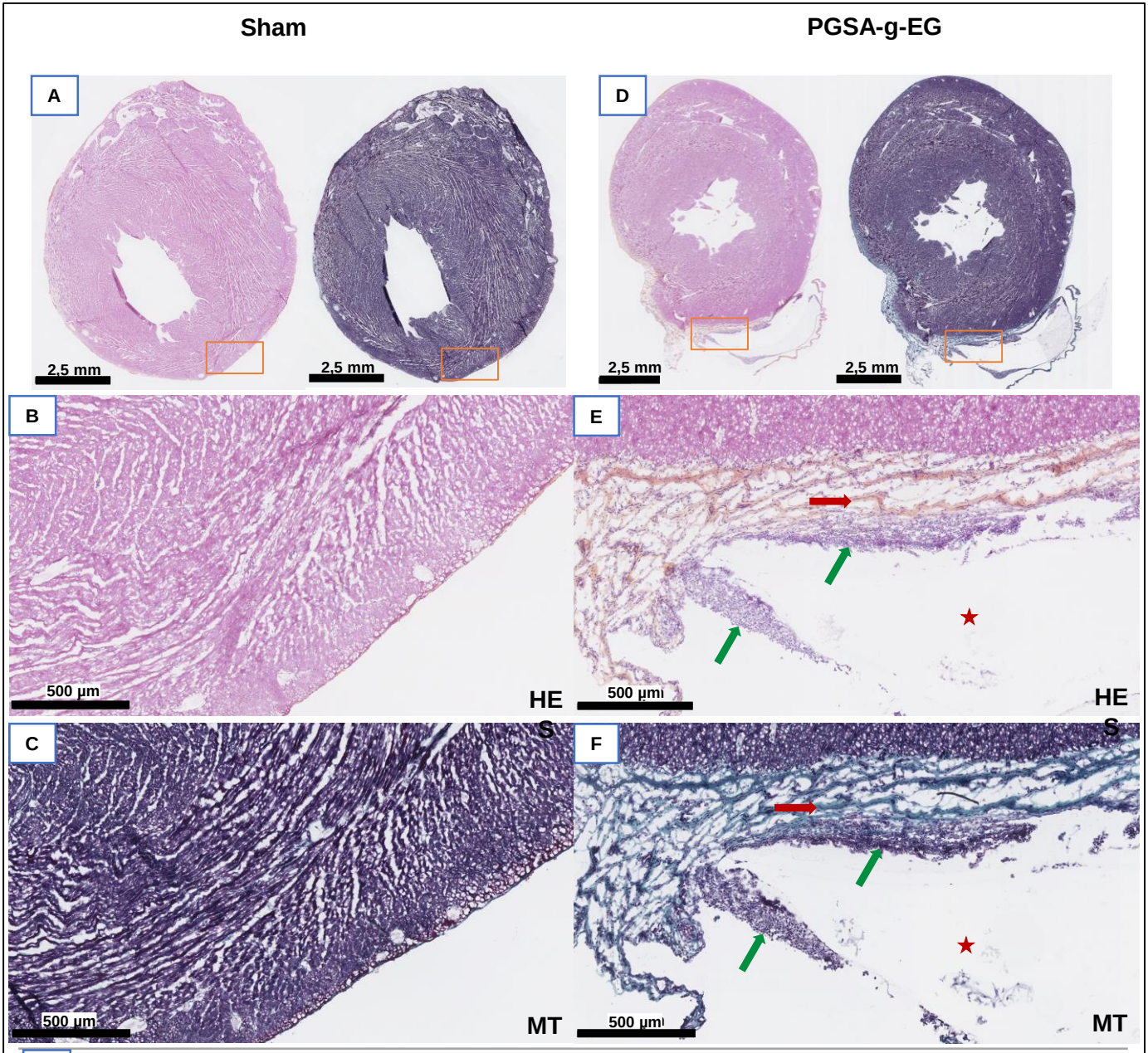

G

	Sham			PGSA-g-EG polymer		
Animal number	Animal 1	Animal 2	Animal 3	Animal 1	Animal 2	Animal 3
Inflammation (mononuclear cells)	NS	NS	NS	NS	Grade 2	Grade 1
Fibrosis	NS	NS	NS	Grade 2	Grade 1	Grade 1

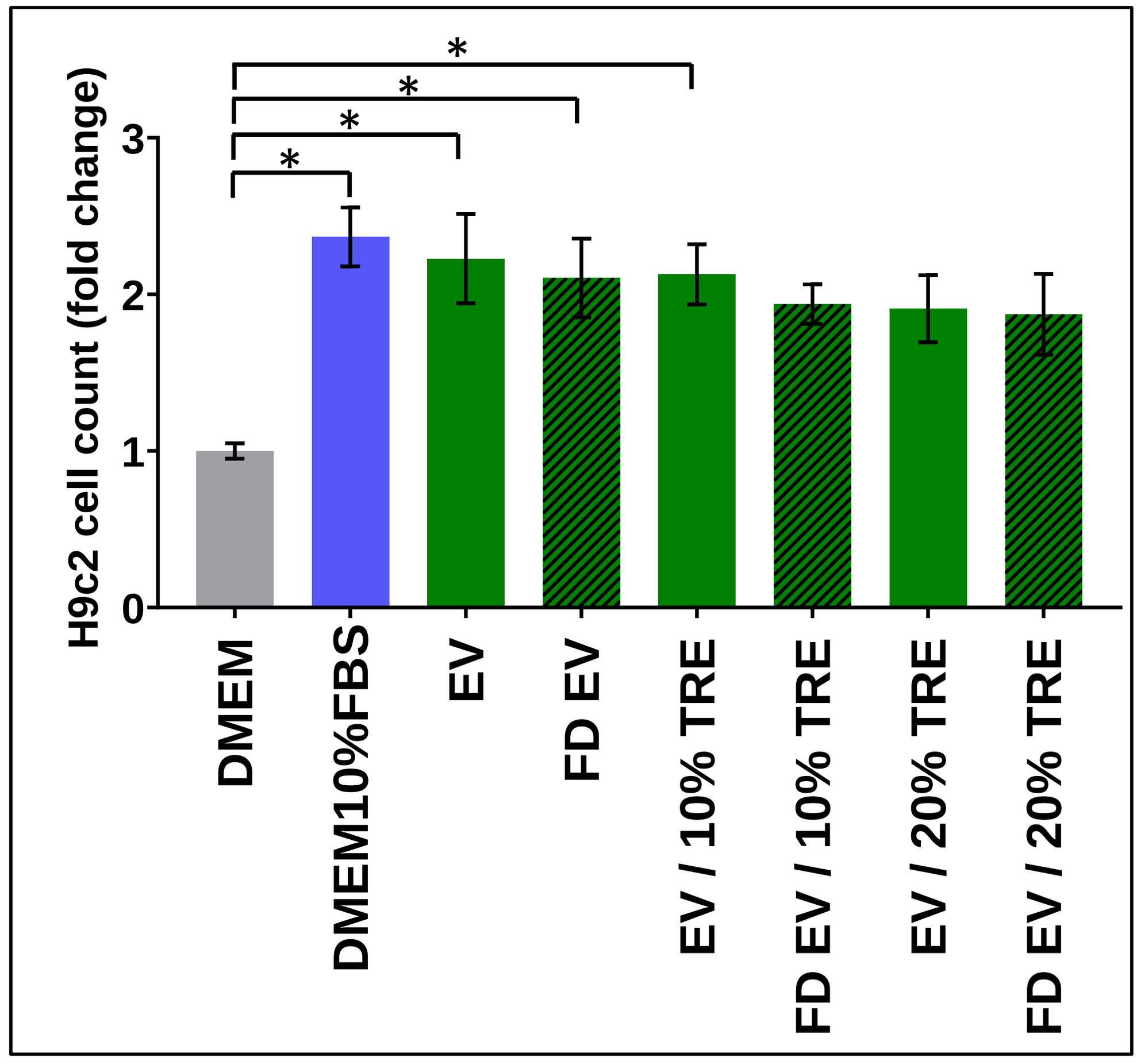
H9c2 cell count (fold change)
0
1
2
3
*
*
*
*
*
DMEM
DMEM10%FBS
EV
FD EV
EV / 10% TRE
FD EV / 10% TRE
EV / 20% TRE
FD EV / 20% TRE

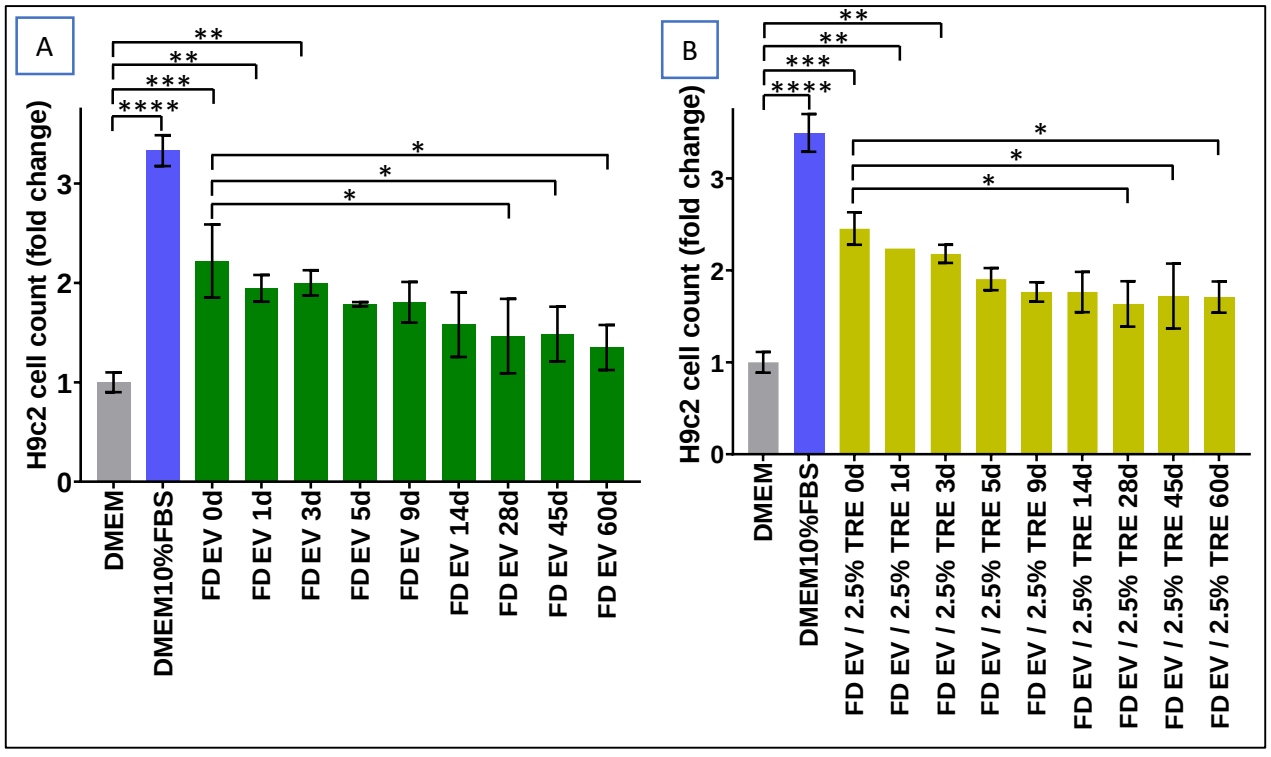
A
H9c2 cell count (fold change)
0
1
2
3
****
***
**
**
*
*
*
DMEM
DMEM10%FBS
FD EV 0d
FD EV 1d
FD EV 3d
FD EV 5d
FD EV 9d
FD EV 14d
FD EV 28d
FD EV 45d
FD EV 60d
B
H9c2 cell count (fold change)
0
1
2
3
****
***
**
**
*
*
*
DMEM
DMEM10%FBS
FD EV / 2.5% TRE 0d
FD EV / 2.5% TRE 1d
FD EV / 2.5% TRE 3d
FD EV / 2.5% TRE 5d
FD EV / 2.5% TRE 9d
FD EV / 2.5% TRE 14d
FD EV / 2.5% TRE 28d
FD EV / 2.5% TRE 45d
FD EV / 2.5% TRE 60d

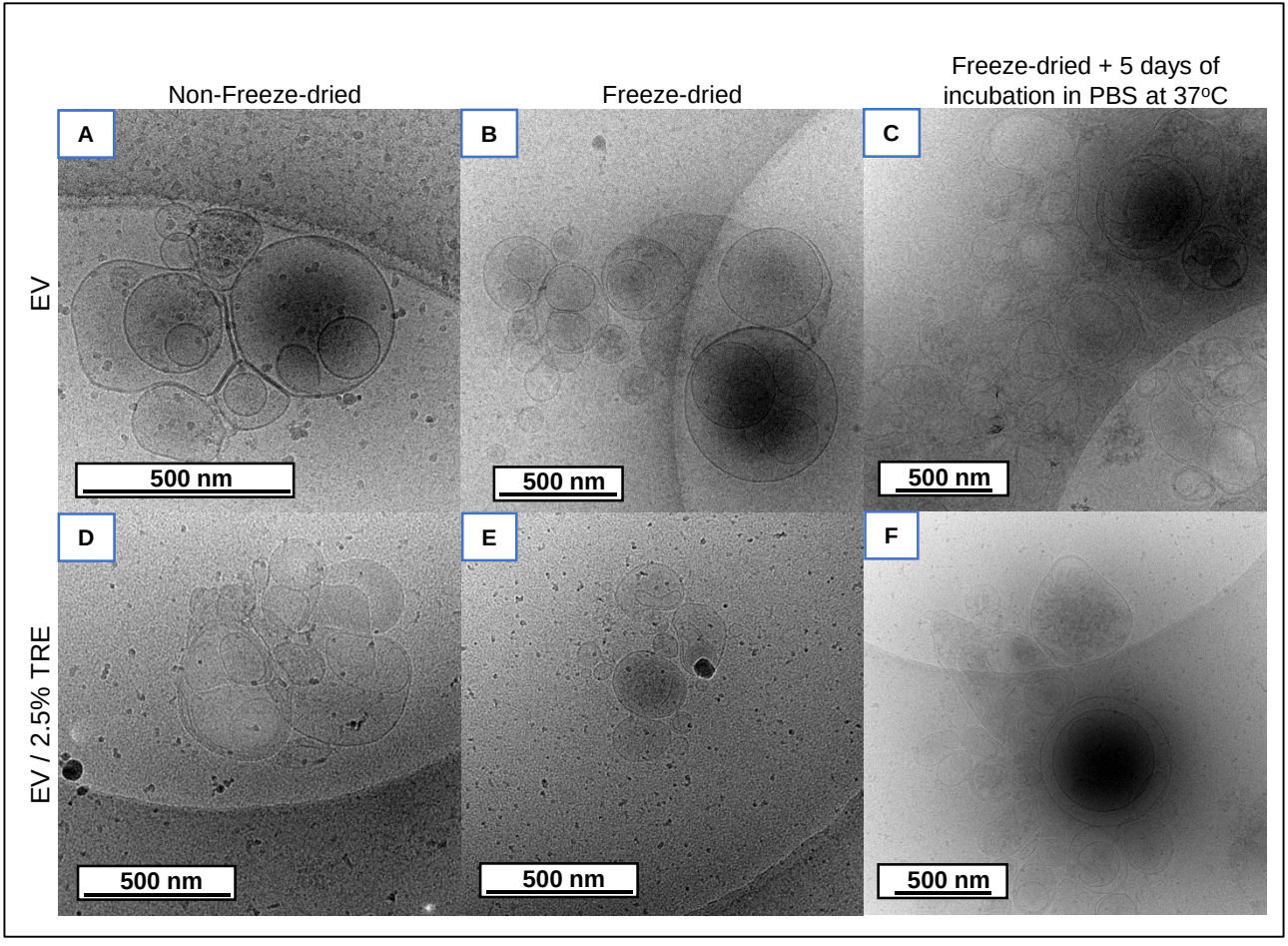
Non-Freeze-dried
Freeze-dried
Freeze-dried + 5 days of incubation in PBS at 37ºC
EV
EV / 2.5% TRE
A
B
C
D
E
F
500 nm
500 nm
500 nm
500 nm
500 nm
500 nm

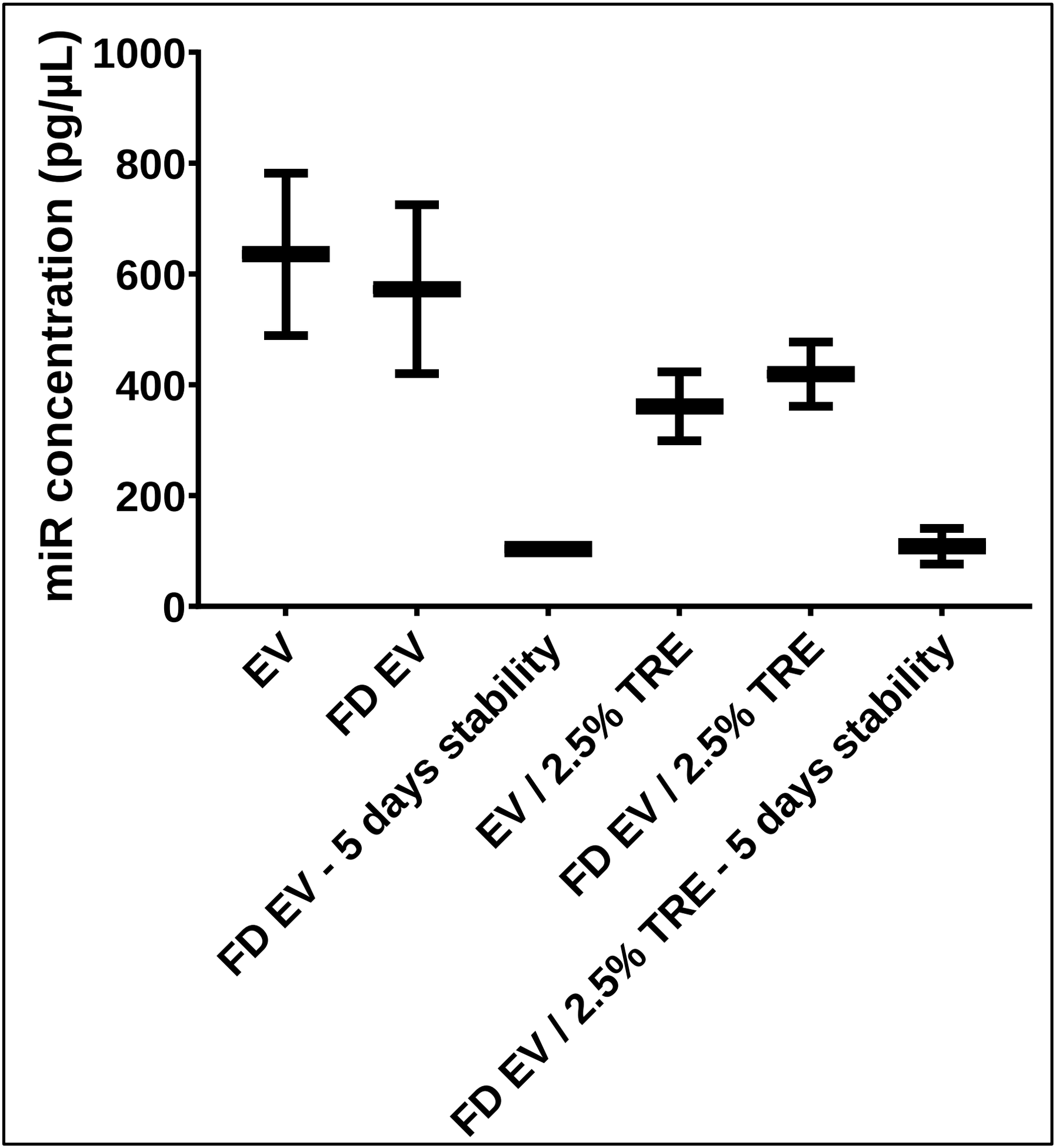
miR concentration (pg/µL)
1000
800
600
400
200
0
EV
FD EV
FD EV - 5 days stability
EV / 2.5% TRE
FD EV / 2.5% TRE
FD EV / 2.5% TRE - 5 days stability

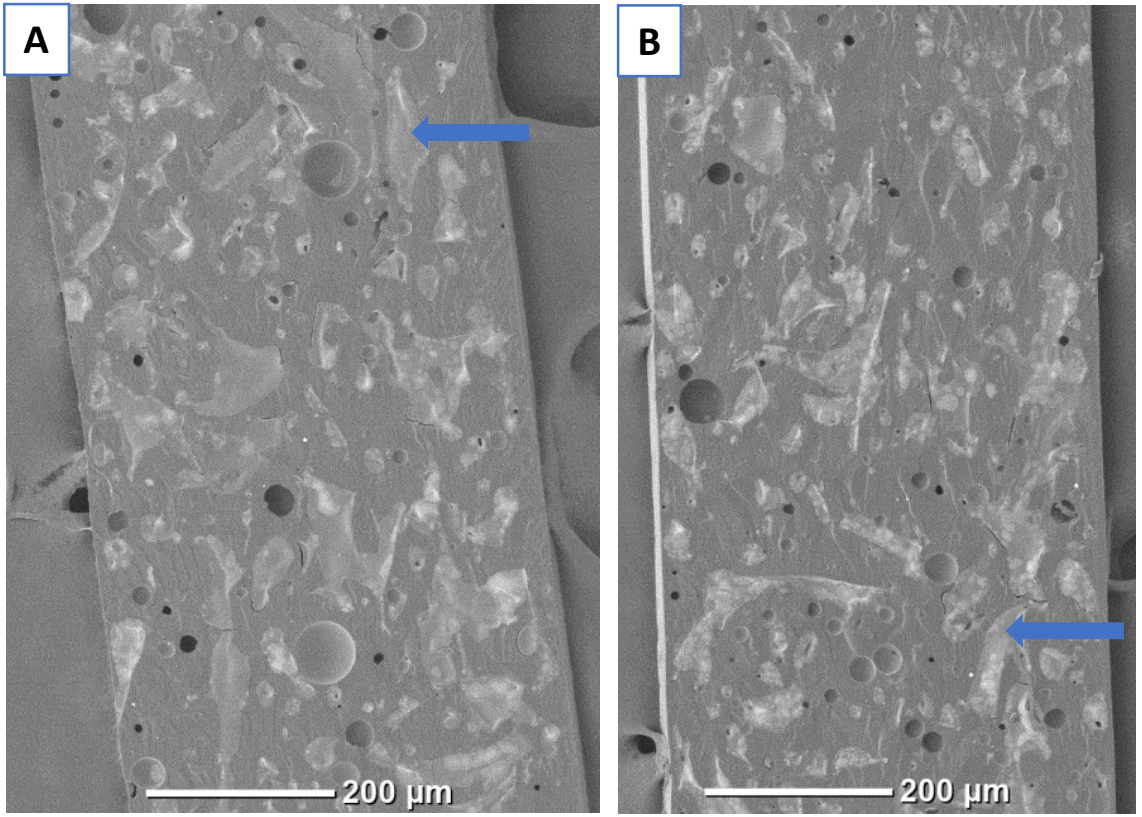
A
200 µm
B
200 µm

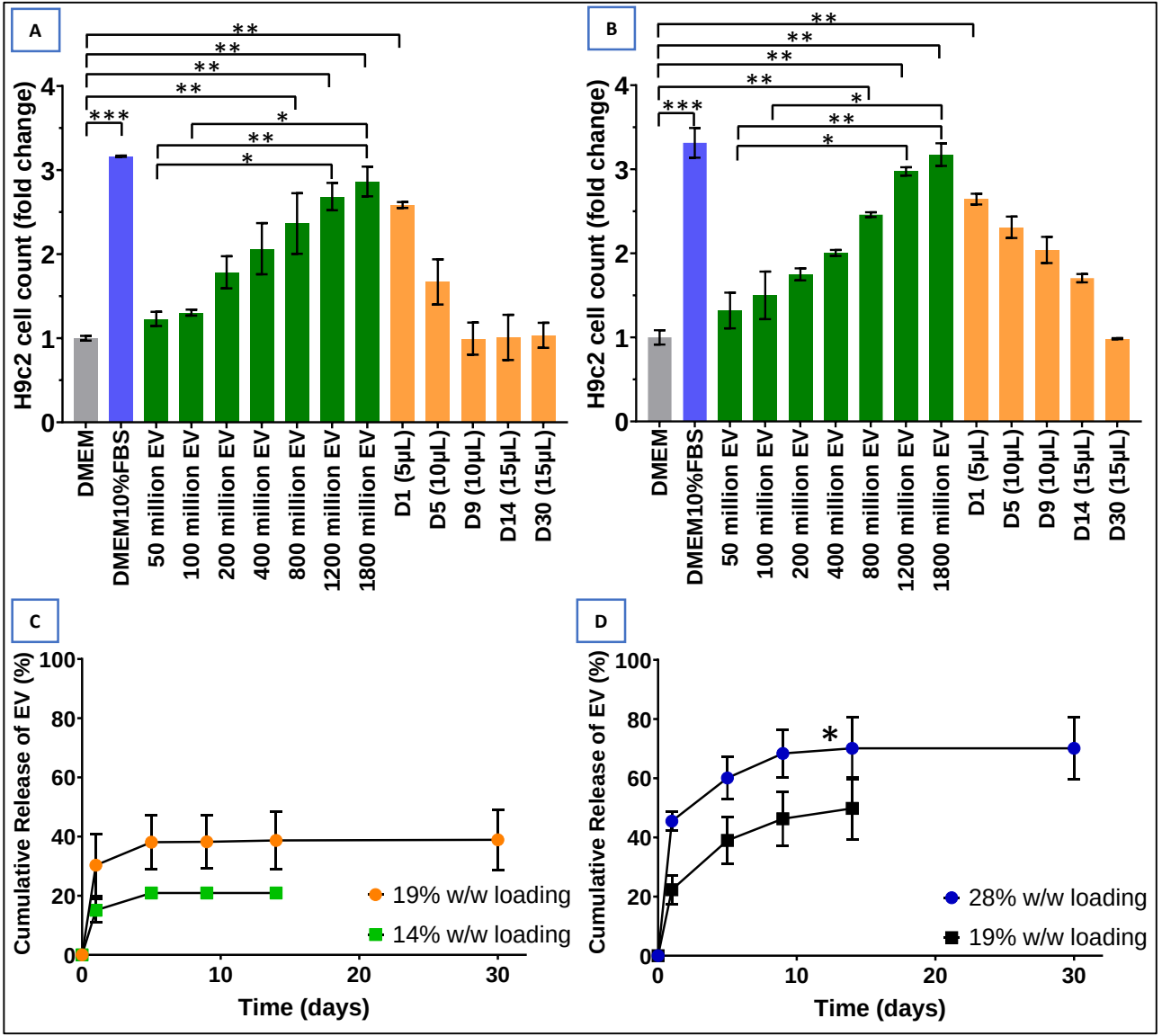
A
H9c2 cell count (fold change)
DMEM
DMEM10%FBS
50 million EV
100 million EV
200 million EV
400 million EV
800 million EV
1200 million EV
1800 million EV
D1 (5µL)
D5 (10µL)
D9 (10µL)
D14 (15µL)
D30 (15µL)
B
H9c2 cell count (fold change)
C
Cumulative Release of EV (%)
19% w/w loading
14% w/w loading
Time (days)
D
Cumulative Release of EV (%)
28% w/w loading
19% w/w loading
Time (days)

Adhesive patch based on PGSA-g-EG polymer

Freeze-dried Extracellular Vesicles derived from iPSC-Pg

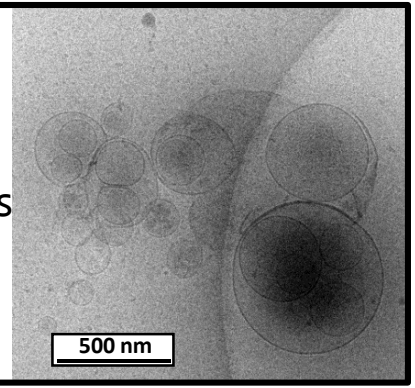

Controlled released of extracellular vesicles for cardiac repair